JACS
JOURNAL OF THE AMERICAN CHEMICAL SOCIETY
Article
pubs.acs.org/JACS

Protein Activity Regulation: Inhibition by Closed-Loop Aptamer-Based Structures and Restoration by Near-IR Stimulation

Jie Wang,[†,§] Yurong Wei,[†,‡,§] Xiaoxia Hu,[†] Yu-Yan Fang,[†] Xinyang Li,[†] Jian Liu,[†] Shengfu Wang,[‡] and Quan Yuan*[,†]

[†]Key Laboratory of Analytical Chemistry for Biology and Medicine (Ministry of Education), College of Chemistry and Molecular Sciences, Wuhan University, Wuhan 430072, China

[‡]Ministry of Education, Key Laboratory for the Synthesis and Application of Organic Functional Molecules & College of Chemistry and Chemical Engineering, Hubei University, Wuhan 430062, China

Supporting Information

ABSTRACT: Regulation of protein activity is vital for understanding the molecular mechanism of biological activities. In this work, protein activity is suppressed by proximity-dependent surface hybridization and subsequently restored by near-infrared (NIR) light stimulation. Specifically, by constructing closed-loop structures with two aptamer-based affinity ligands, significantly enhanced inhibition of thrombin activity is achieved compared to traditional single affinity ligand based inhibitors. Furthermore, the activity of inhibited thrombin is efficiently recovered under NIR light stimulation by using gold nanorods (AuNRs) as photothermal agents to disrupt the closed-loop structures. Real-time and in situ monitoring of the conversion of fibrinogen into fibrin catalyzed by both inhibited and recovered thrombin was performed with light scattering spectroscopy and laser scanning confocal microscopy (LSCM). Thrombin trapped in the closed-loop structures shows slow reaction kinetics, while the photothermally liberated thrombin displays largely recovered catalytic activity. Human plasma was further employed to demonstrate that both the inhibited and restored thrombin can be applied to clotting reaction in reality. This strategy provides protein activity regulation for studying the molecular basis of biological activities and can be further applied to potential areas such as metabolic pathway regulation and the development of protein-inhibitor pharmaceuticals.

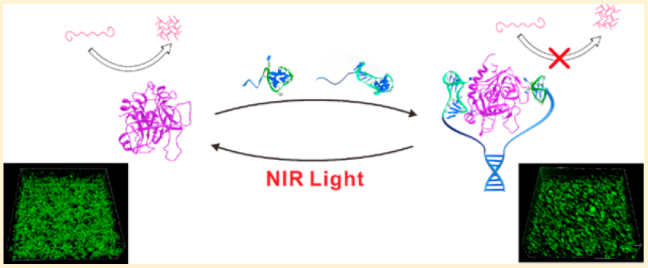

INTRODUCTION

Proteins are the main performers of life activities, and nearly all biological processes involve the precise regulation of protein activity to accomplish specific tasks. These regulation processes usually arise from blocking or altering the active domains of proteins in response to various internal signals.[1] During the past several decades, the use of external signals to inhibit and restore protein activity has attracted considerable attention. Such studies aid in understanding the molecular mechanisms of biological processes, and they are also important in areas such as metabolic pathway regulation, drug development and biocatalysis.[2] In recent years, a variety of compounds that can bind to proteins and interfere with their activity have been developed,[3] and studies of the regulatory functions of these molecules in proteins have yielded encouraging results.[4] A major focus in these studies is improvement of the binding specificity and affinity of the compound to the protein to achieve potent inhibitory capabilities.[3a,5] On the other hand, many of the molecular-based inhibition processes are restricted to the active sites of proteins and are usually nonreversible, leading to so-called suicide inhibition.[4f,6] As a consequence, it is of great significance to develop novel methods for robust protein inhibition, as well as efficient restoration of protein activity.

In recent years, aptamers have emerged as a new class of DNA molecules which specifically bind to targets with dissociation constants (K_d) in the picomolar to nanomolar range[7] by folding into unique secondary or tertiary structures that accommodate the target's molecular structure.[8] Aptamers that can specifically bind to proteins and inhibit their activity have already been reported.[9] Hence, aptamers are potential molecules for regulation of protein activity. Proximity-dependent surface hybridization is a novel DNA nanotechnology developed by Landegren and co-workers.[10] They discovered that coordinated and proximal binding of two aptamers to the same target to form a closed-loop structure could promote the ligation of oligonucleotides linked to each aptamer by increasing the local concentration.[11] Recently, Le and co-workers have developed many novel binding-induced DNA strand displacement assays based on proximity-dependent surface hybridization for ultrasensitive detection of proteins.[12] More importantly, they observed that formation of the highly stable closed-loop structure could raise the melting temperature (T_m) of the hybrid by more than 30 °C.[13] These studies indicated that the closed-loop structure greatly enhances the

Received: May 11, 2015
Published: August 10, 2015

DOI: 10.1021/jacs.5b04894
J. Am. Chem. Soc. 2015, 137, 10576−10584

Scheme 1. Schematic Representation of Thrombin Inhibition by the Closed-Loop Structure and Subsequent Release of Thrombin by NIR Light Stimulation

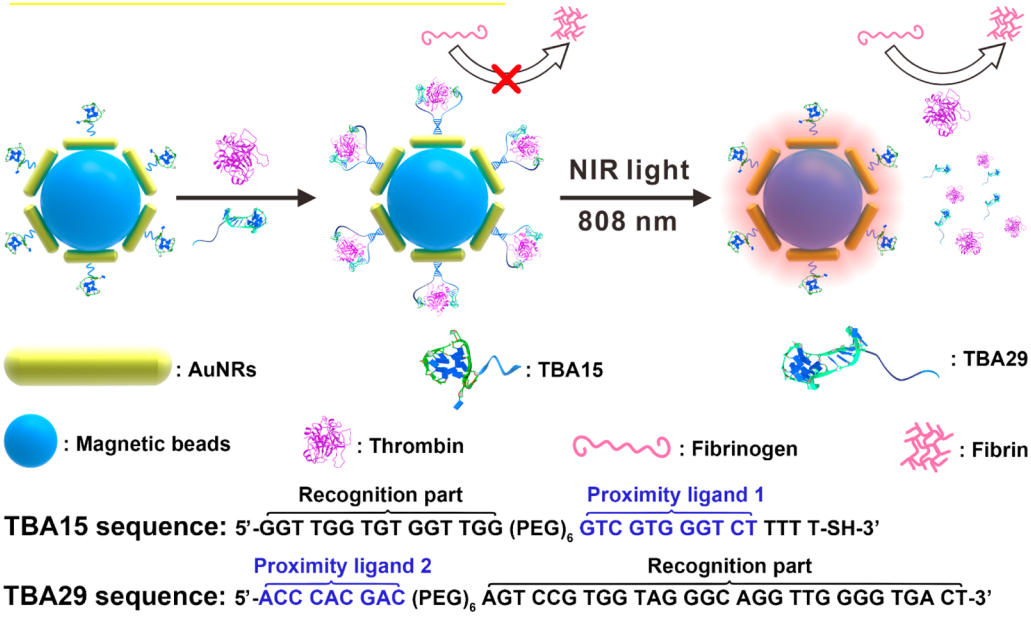

binding affinity of ligands such as aptamers.[14] In addition, formation of the closed-loop structure can be initiated only when the target protein is recognized by two affinity ligands, thus further improving the binding specificity. Therefore, construction of aptamer-based closed-loop structures with proximity-dependent surface hybridization assay is a promising strategy for the highly specific and robust inhibition of protein activity.

Photocontrol of protein activity has been studied by several research groups.[15] In their review of this topic, Mayer and co-workers showed that, compared to other approaches, photons offer pronounced advantages, including high spatial and temporal control.[16] However, despite the achievements on caged and light-switchable proteins mentioned in Mayer's review, further efforts should be made to provide milder strategies, especially considering the tissue damage associated with UV light and the complicated procedure to prepare caged proteins. Usually, long-wavelength, especially near-infrared (NIR), light is preferred for protein activity regulation since it allows deep tissue penetration with little photodamage, in addition to submicrometric resolution in three dimensions.[17] For instance, Schifferli et al. have reported an elegant approach in which NIR light was employed for the controlled release of anticoagulant and antidote for on/off switching of blood clotting.[18] Use of NIR photons to restore protein activity inhibited by potent aptamer-based closed-loop structures can be achieved by conversion of radiant energy to heat. Noble metal nanoparticles, such as gold nanorods (AuNRs), are efficient photothermal agents due to their unique localized surface plasmon resonance (LSPR) properties.[19] Furthermore, the 3D structure of aptamers is highly sensitive to temperature variations. Accordingly, proteins trapped in aptamer-based closed-loop structures can be liberated by NIR irradiation using AuNRs as the photothermal medium.

This paper describes significantly enhanced inhibition of protein activity with aptamer-based affinity ligands by proximity-dependent surface hybridization assay. Subsequent NIR irradiation liberates the proteins trapped in the closed-loop structures using the LSPR property of AuNRs. Thrombin was chosen as the model protein because of its critical role in the blood clotting process. Another important factor is the availability of two thrombin binding aptamers (15-base and 29-base oligonucleotides, designated as TBA15 and TBA29, respectively) that bind at different sites (exosite 1 and exosite 2). According to previous studies, TBA15 can inhibit the activity of thrombin but the binding affinity is modest (K_d, ~100 nM),[9] and TBA29 exhibits little inhibiting capability toward thrombin but has strong binding affinity (K_d, ~0.5 nM).[20] With proximity-dependent surface hybridization, greatly enhanced inhibitory performance toward thrombin is obtained via the synergistic effect elicited by TBA15 and TBA29 in the closed-loop structure. Furthermore, the activity of inhibited thrombin can be recovered using NIR light stimulation. The schematic representation of the principle is outlined in Scheme 1. AuNRs are immobilized on magnetic beads (designated as MB/Au) and thiol-labeled TBA15 is assembled on the AuNR surfaces (designated as MB/AuNRs-TBA15). With the addition of TBA29 and thrombin, the two aptamers specifically bind to thrombin, and proximity ligand 1 at the 3′ end of TBA15 hybridizes with proximity ligand 2 at the 5′ end of TBA29 to form DNA duplexes. Formation of the closed-loop structure inhibits the catalytic activity of thrombin in the conversion of fibrinogen into fibrin. When NIR light (808 nm) is applied, AuNRs effectively convert the incident photons into heat to disrupt the closed-loop structure. As a result, the trapped thrombin is released and its catalytic activity is restored. In addition, the MB/AuNRs-TBA15 complex can be isolated from the solution with a permanent magnet for further use in the next inhibition test. This strategy provides protein activity regulation for studying the molecular basis of biological activities and can be further applied to potential areas such as metabolic pathway regulation and the development of protein-inhibitor pharmaceuticals.

DOI: 10.1021/jacs.5b04894
J. Am. Chem. Soc. 2015, 137, 10576−10584

RESULTS AND DISCUSSION

The feasibility of formation of the closed-loop structure by TBA15, TBA29, and thrombin was tested first with a binding-induced DNA strand displacement assay. As shown in Figure 1a, TBA15 was immobilized on the surface of AuNRs and

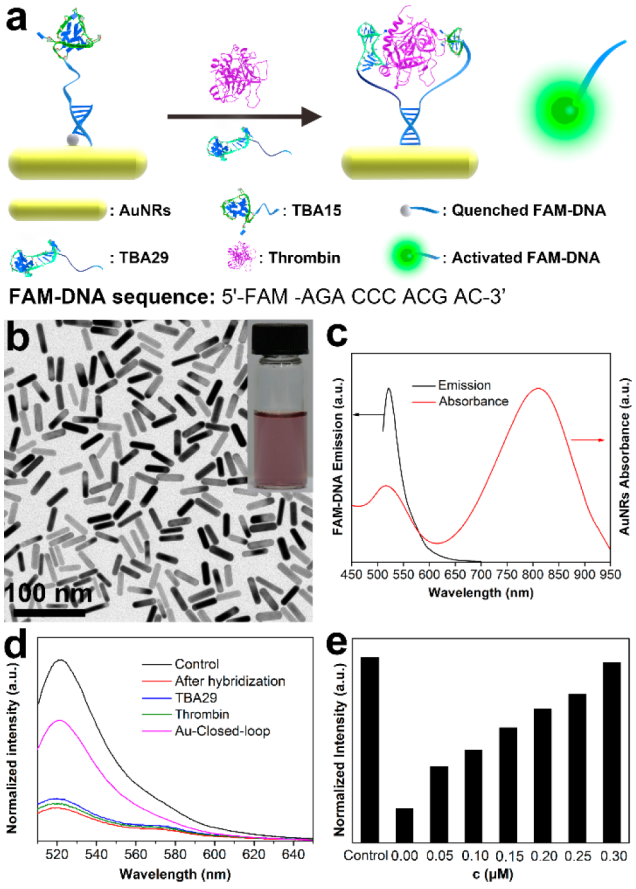

Figure 1. (a) Schematic illustration of the binding-induced DNA strand displacement assay. (b) TEM image of AuNRs. Scale bar, 100 nm. (c) Absorption spectrum of AuNRs and fluorescence spectrum of FAM-DNA. (d) Fluorescence spectra of FAM-DNA before (Control) and after hybridization with TBA15; and with addition of TBA29 and thrombin separately or simultaneously. (e) Increase of fluorescence intensity as a function of the thrombin concentration.

FAM-DNA was hybridized to proximity ligand 1 at the 3′ end of TBA15 to form a stable TBA15/FAM-DNA duplex (T_m, ~40 °C), resulting in quenching of the fluorescence. In the presence of TBA29 and thrombin, the binding of thrombin to TBA15 and TBA29 brings ligand 2 at the 5′ end of TBA29 into close proximity to ligand 1, which induces the strand-displacement reaction between TBA29 and FAM-DNA. As a result, TBA15/TBA29 duplex forms and FAM-DNA is released from the AuNRs, leading to recovery of fluorescence. It is noteworthy that the complementary sequence in the TBA15/FAM-DNA duplex is 2 nucleotides longer than that of the TBA15/TBA29 duplex to minimize the displacement of FAM-DNA by TBA29 in the absence of thrombin. The transmission electron microscopy (TEM) image of AuNRs and a photograph of the AuNRs solution are presented in Figure 1b and Figure S1. AuNRs are well dispersed with aspect ratio of about 3.8 (38 × 10 nm). The UV−vis absorption spectrum of AuNRs and the emission spectrum of FAM-DNA are shown in Figure 1c. AuNRs display two absorption bands at around 520 and 810 nm due to the transverse and longitudinal SPR. Absorption at 520 nm quenches the fluorescence of FAM-DNA, whose emission peak is centered at 520 nm. The 810 nm absorption converts NIR photons into heat. Figure 1d presents the results of the binding-induced DNA strand displacement assay. The fluorescence emission of FAM-DNA is quenched after hybridization with TBA15 on the surface of AuNRs. In the presence of either TBA29 or thrombin alone, little change in the fluorescence intensity occurs, indicating that, by themselves, neither TBA29 nor thrombin can initiate the strand displacement reaction. However, with simultaneous addition of both TBA29 and thrombin, the fluorescence is largely recovered, indicating that the closed-loop structure was successfully formed (T_m > 40 °C). In addition, by fixing the amounts of TBA29, the emission intensities of FAM-DNA increase gradually with increasing thrombin concentration (Figure 1e and Figure S6), clearly demonstrating the tendency of TBA15, TBA29, and thrombin to form the designed closed-loop structure.

The strategy for real-time monitoring of the conversion of fibrinogen into fibrin catalyzed by thrombin is illustrated in Figure 2a. Fibrinogen is dissolved in solution and the light

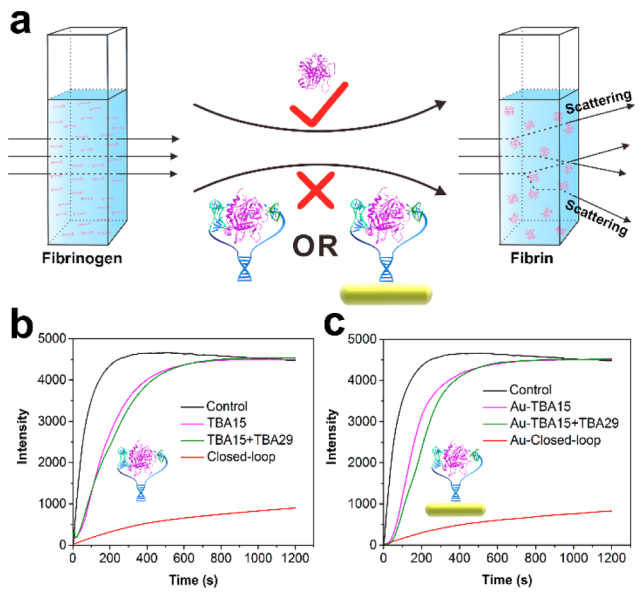

Figure 2. (a) Inhibition of thrombin catalytic activity in conversion of fibrinogen into fibrin. (b) Real-time light scattering spectra of fibrinogen solution with added thrombin (Control), thrombin inhibited by TBA15, by TBA29 and TBA15 without the proximity ligands (TBA15 + TBA29), and by the closed-loop structure. (c) Real-time light scattering spectra of fibrinogen solution treated with thrombin (Control), thrombin inhibited by Au-TBA15, by Au-TBA15 and TBA29 without the proximity ligands (Au-TBA15 + TBA29) inhibited thrombin, and by the Au-Closed-loop structure.

scattering signals are weak. In the presence of thrombin, fibrinogen is rapidly converted into insoluble fibrin fibers, leading to significant enhancement of the scattering signal. When thrombin is trapped in the closed-loop structure, the catalytic conversion of fibrinogen is inhibited. The inhibitory performance of the closed-loop structure formed in the absence of AuNRs (designated as Closed-loop) was tested first and the results are shown in Figure 2b. Fibrinogen solution with added thrombin shows rapid reaction kinetics, and the scattering

DOI: 10.1021/jacs.5b04894
J. Am. Chem. Soc. 2015, 137, 10576−10584

intensity quickly reaches a plateau. Samples treated with TBA15-inhibited thrombin require a little longer time to reach the plateau, in accordance with a previous study.[15e] When TBA29 and TBA15 without the proximity ligands are simultaneously added to the fibrinogen solution, only a slightly enhanced inhibitory performance is observed, since the closed-loop structure cannot form. However, for the fibrinogen solution treated with the closed-loop structure, the scattering signals increase very slowly and the final scattering intensity is much lower than that of the former three samples. These results clearly demonstrate that the inhibition capabilities of a single affinity ligand-based inhibitor can be greatly enhanced by forming the closed-loop structure, in which two affinity ligands elicit a potent synergistic effect. When AuNRs are further utilized as the scaffold for the formation of the closed-loop structure (designated as Au-Closed-loop), similar results are obtained (Figure 2c). Thrombin inhibited by Au-TBA15 or by Au-TBA15 and TBA29 without the proximity ligands show rapid reaction kinetics. However, the scattering intensity corresponding to trapped thrombin increases very slowly, and the final scattering intensity is even lower than that of the Closed-loop group (Figure S7). These results indicate that the activity of thrombin can be efficiently inhibited by the closed-loop structure.

To obtain more detailed information about the inhibition efficiency of the single affinity ligand-based inhibitor and the closed-loop structures, the activity of thrombin for the clotting of fibrinogen were further measured, as shown in Table 1. The

Table 1. Activity of Thrombin for the Clotting of Fibrinogen[a]

samples	thrombin activity (%)
Control	100
TBA15	50.8
TBA15+TBA29	43.1
Closed-loop	4.67
Au-TBA15	61.4
Au-TBA15+TBA29	46.9
Au-Closed-loop	4.11

[a]The activity of uninhibited thrombin is defined as 100%.

activity of thrombin in the absence of any inhibitor is defined to be 100%. Most notably, the activity of thrombin trapped by both the Closed-loop and Au-Closed-loop structure are all below 5%, much lower than that of thrombin inhibited by TBA15 (50.8%) or Au-TBA15 (61.4%), suggesting that the closed-loop structure possesses much stronger inhibition efficiency than a single affinity ligand based inhibitor. Beyond that, the activity of thrombin inhibited by two TBAs without the proximity ligands (43.1% and 46.9%, respectively) is much higher than that of the closed-loop structures trapped thrombin (4.67% and 4.11%, respectively), which clearly indicates that forming the designed closed-loop structure can achieve significantly improved inhibition efficiency toward thrombin.

The process of catalytic conversion of fibrinogen into fibrin was further monitored in situ by laser scanning confocal microscopy (LSCM). Fibrinogen, which was labeled with Alexa Fluor 488, would be converted into fluorescent fibrin fibers in the presence of thrombin. Figure 3a and Figure S11 show the dynamic morphological changes of fibrinogen treated with thrombin. At t = 1 min, a large number of small flocculent fibrin fibers are observed due to the rapid aggregation of fibrinogen by the excellent catalytic activity of thrombin. Images at the following time intervals suggest that the small fibrin fibers continue to aggregate into larger fibrin fibers that can be easily visualized even at t = 7 min (dynamic process is shown in Video S1). TBA15 was employed to inhibit thrombin activity, and the images are presented in Figure 3b. Only fibrin oligomers are observed at t = 1 min, indicating that the activity of thrombin is inhibited by TBA15. The fibrin oligomers aggregate into larger fibrin fibers, which are recognizable at t = 7 min (Figure S12 and Video S1). As for fibrinogen solution treated with Au-Closed-loop, a much slower conversion rates is observed (Figure 3c, Figure S14 and Video S1). Fibrin oligomers appear in the first 13 min but small fibrin fibers are not recognizable until t = 19 min, indicating the efficient inhibition of thrombin activity by the closed-loop structure. The small fibrin fibers tend to aggregate with rather slow kinetics compared to the former two groups, as shown by images taken at subsequent timeintervals. The differences between the LSCM images were further analyzed by quantifying the average fluorescence intensity of the images with the image processing software. Results show that the average intensity of TBA15-inhibited thrombin is close to that of the uninhibited thrombin (Figure S15). However, the intensity indexed to Au-Closed-loop is much lower than that of uninhibited thrombin, indicating that Au-Closed-loop displayed stronger inhibition efficiency than TBA-15. Z-stack images of the above samples at t = 60 min were obtained and 3D surface projection of Z-stack images was employed to show the density and distribution of fibrin fibers in each sample. As shown in Figure 3d, fibrinogen treated with thrombin shows a high density of fibrin networks (Video S2). Figure 3e indicates that the density of fibrin fibers in a sample exposed to TBA15-inhibited thrombin is lower than that of fibrinogen solution treated with uninhibited thrombin (Video S2). Figure 3f shows the fibrinogen solution treated with Au-Closed-loop. It is obvious that the density and size of fibrin fibers are much smaller than those in the former two groups (Video S2). The above results therefore vividly demonstrate that, compared to a traditional single aptamer inhibitor, greatly enhanced inhibitory ability is obtained by constructing the closed-loop structure.

The inhibition of thrombin activity was also characterized by light microscopy (LM). Photographs of fibrinogen solutions treated with both uninhibited and inhibited thrombin for 30 min are presented in Figure 4. Dense and huge fibrin networks are observed after treating fibrinogen solution with thrombin (Figure 4a and Figure S18). As for TBA15-inhibited thrombin (Figure 4b and Figure S19), loose fibrin networks are observed. Figure 4c shows fibrinogen solution treated with Au-Closed-loop and only a few fibrin fibers are observed (Figure S20). These results again demonstrate that the closed-loop structure provides significantly enhanced inhibitory ability toward thrombin.

The outstanding performance of proximity-dependent surface hybridization assay in suppressing thrombin activity has been clearly demonstrated. Next, the feasibility of NIR light triggered restoration of activity was further investigated. AuNRs were immobilized on the surface of magnetic beads (MBs) in order to isolate MB/Au-TBA15 from the solution after photothermal treatment (Figure S25). The closed-loop structure (designated as MB/Au-Closed-loop) was formed by adding MB/Au-TBA15 to the solution containing TBA29 and thrombin. The schematic representation of the strategy to restore thrombin activity is shown in Figure 5a. MB/Au-

DOI: 10.1021/jacs.5b04894
J. Am. Chem. Soc. 2015, 137, 10576−10584

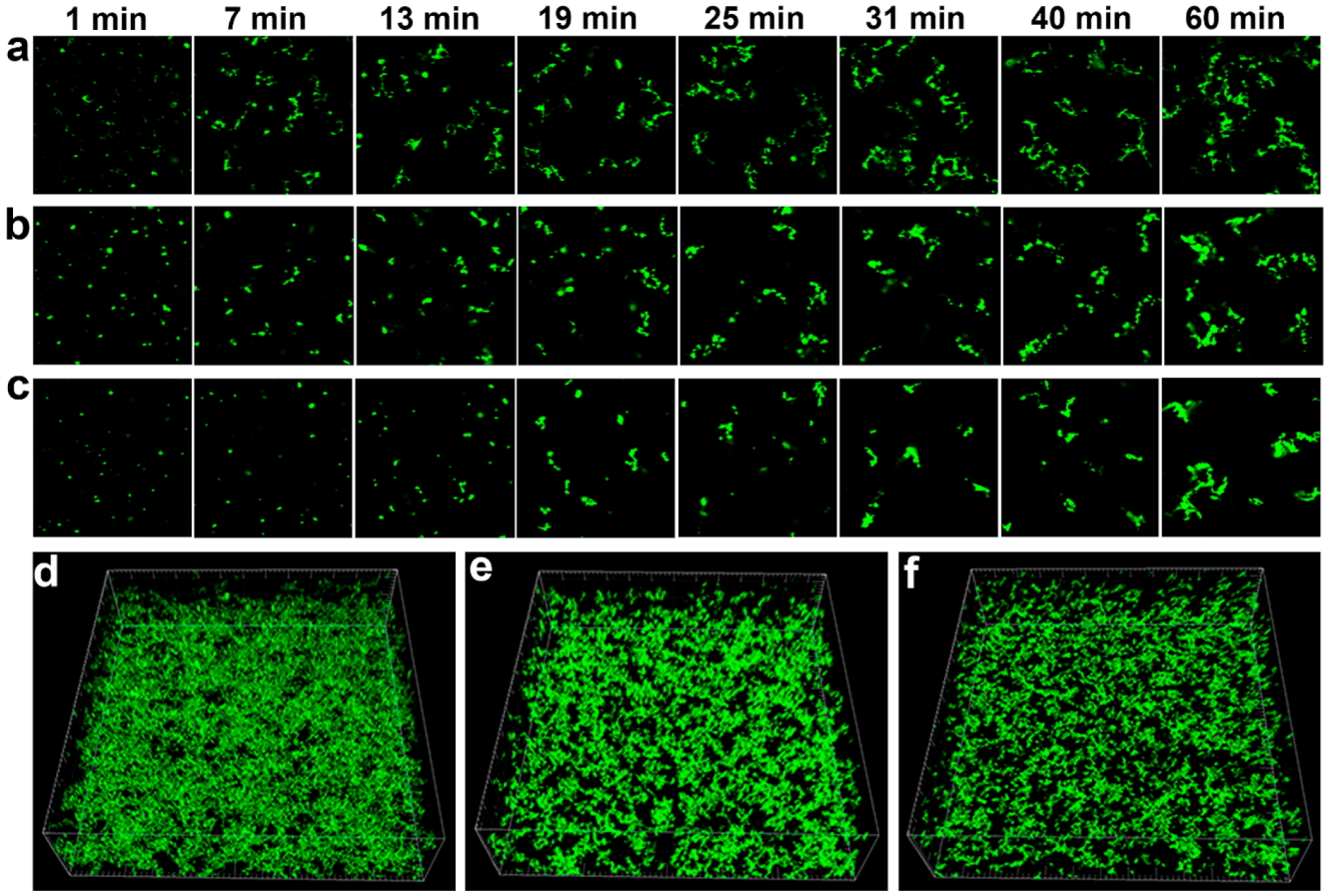

Figure 3. In situ monitoring of the conversion of fibrinogen into fibrin. Dynamic morphology changes of fibrinogen treated with thrombin (a), TBA15-inhibited thrombin (b), and Au-Closed-loop (c). 3D Surface projections of Z-stack images for fibrinogen treated with thrombin (d), TBA15-inhibited thrombin (e), and Au-Closed-loop (f) at t = 60 min.

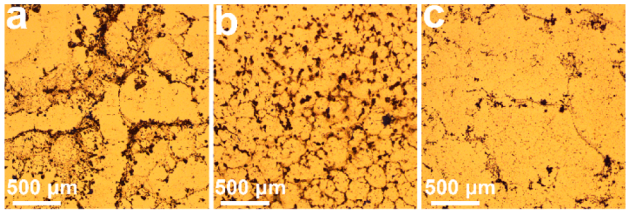

Figure 4. LM images of fibrinogen treated with thrombin (a), TBA15-inhibited thrombin (b), and Au-Closed-loop (c).

Closed-loop effectively inhibits the catalytic activity of thrombin toward the clotting reaction. With increasing temperature, the closed-loop structure is disrupted due to denaturation of TBA15, TBA29 and the stem DNA duplex. The recovered thrombin can efficiently catalyze the conversion of fibrinogen into fibrin, resulting in enhancement of the scattering signals. Since restoration of thrombin activity relies on temperature increase, MB/Au-Closed-loop solutions were heated to different temperatures with a constant temperature bath to investigate the recovery rates of thrombin activity. As mentioned above, the T_m of the closed-loop structure is higher than 40 °C; hence, this value was set as the lowest temperature in this test. The activity of thrombin restored by treating MB/Au-Closed-loop at different temperatures is presented in Figure 5b. As expected, thrombin activity is significantly inhibited in MB/Au-Closed-loop structures, and little change is observed after treating MB/Au-Closed-loop solution at 40 °C. The activity of thrombin first increases with increasing temperature, and then decreases gradually at temperatures above 60 °C. The activity of thrombin liberated at different temperatures was investigated (Table S2). Thrombin restored by treating the MB/Au-Closed-loop structure at 60 °C showed the highest activity. On the basis of these results, 60 °C was chosen as the optimized value for the recovery of trapped thrombin. Moreover, the effect of temperature on the activity of thrombin was also studied (Figure S32 and Table S3). After treatment at 60 °C for 10 min, thrombin still retained nearly 90% of its original activity, indicating that thrombin was not significantly damaged by 60 °C treatment. NIR light stimulated liberation of thrombin activity was performed by treating MB/Au-Closed-loop solution with NIR light to increase the temperature of the solution to 60 °C. As shown in Figure 5c, the catalytic activity of thrombin is significantly recovered since a drastic jump in the scattering signal is observed, clearly implying that photo-controlled liberation of thrombin activity is successfully realized by utilizing AuNRs as the photothermal medium. Furthermore, the efficiency of NIR light triggered release of thrombin was determined to be 70.3%. The incomplete release of thrombin may be ascribed to the nonspecific adsorption of thrombin on the surface of MBs particles.[21] Moreover, the activity of photo liberated thrombin was compared to that of the uninhibited thrombin at the same concentrations (Figure S35 and Table S7). The results suggest that the activity of thrombin can be recovered by about 84%, revealing the high efficiency of phototriggered restoration of thrombin activity.

DOI: 10.1021/jacs.5b04894
J. Am. Chem. Soc. 2015, 137, 10576−10584

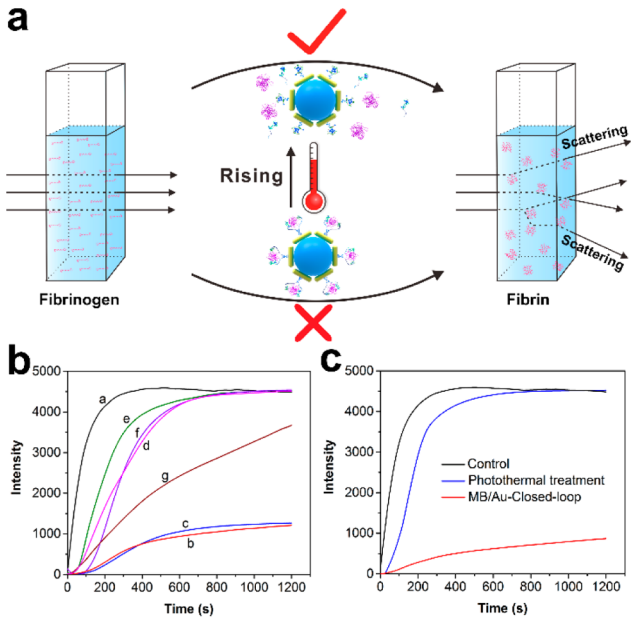

Figure 5. (a) Schematic illustration of restoration of thrombin activity by elevated temperature. (b) Real-time light scattering spectra of fibrinogen solution treated with thrombin recovered at different temperatures (a, Control; b, MB/Au-Closed-loop; c, 40 °C; d, 50 °C; e, 60 °C; f, 70 °C; g, 80 °C). (c) Real-time light scattering spectra of fibrinogen solutions with thrombin (Control), MB/Au-Closed-loop, and photo liberated thrombin.

The activity of photo liberated thrombin was also studied by LSCM. For fibrinogen solution treated with MB/Au-Closed-loop (Figure 6a, Figure S38 and Video S3), typical inhibition of thrombin activity is observed. Small fibrin fibers are observed at t = 25 min, and only a few large fibrin fibers can be recognized even at t = 60 min. After photothermal treatment of the MB/Au-Closed-loop structure at 60 °C with NIR light, clotting reactions similar to those of uninhibited thrombin are observed (Figure 6b, Figure S40 and Video S3). Many fibrin oligomers are observed at t = 1 min and fibrin fibers can be easily recognized at t = 7 min. The fibrin fibers rapidly aggregate into larger fibers, as shown by the photographs at different time intervals. Similarly, the average fluorescence intensity of the above LSCM images were also quantified (Figure S41). The average intensity of photo liberated thrombin is much higher than that of the MB/Au-Closed-loop, clearly suggesting that the activity of thrombin is efficiently restored with NIR light stimulation. 3D surface projection of Z-stack images taken from samples treated with MB/Au-Closed-loop inhibited thrombin show a low density of fibrin fibers (Figure 6c and Video S4), suggesting that the catalytic activity of thrombin is significantly inhibited. As for fibrinogen treated with recovered thrombin, large quantities of fibrin networks are observed (Figure 6d and Video S4). These results therefore vividly demonstrate that the catalytic activity of thrombin is successfully restored with NIR light stimulation.

Human plasma samples were further employed for the clotting reaction, and the thrombin clotting time (TCT) was

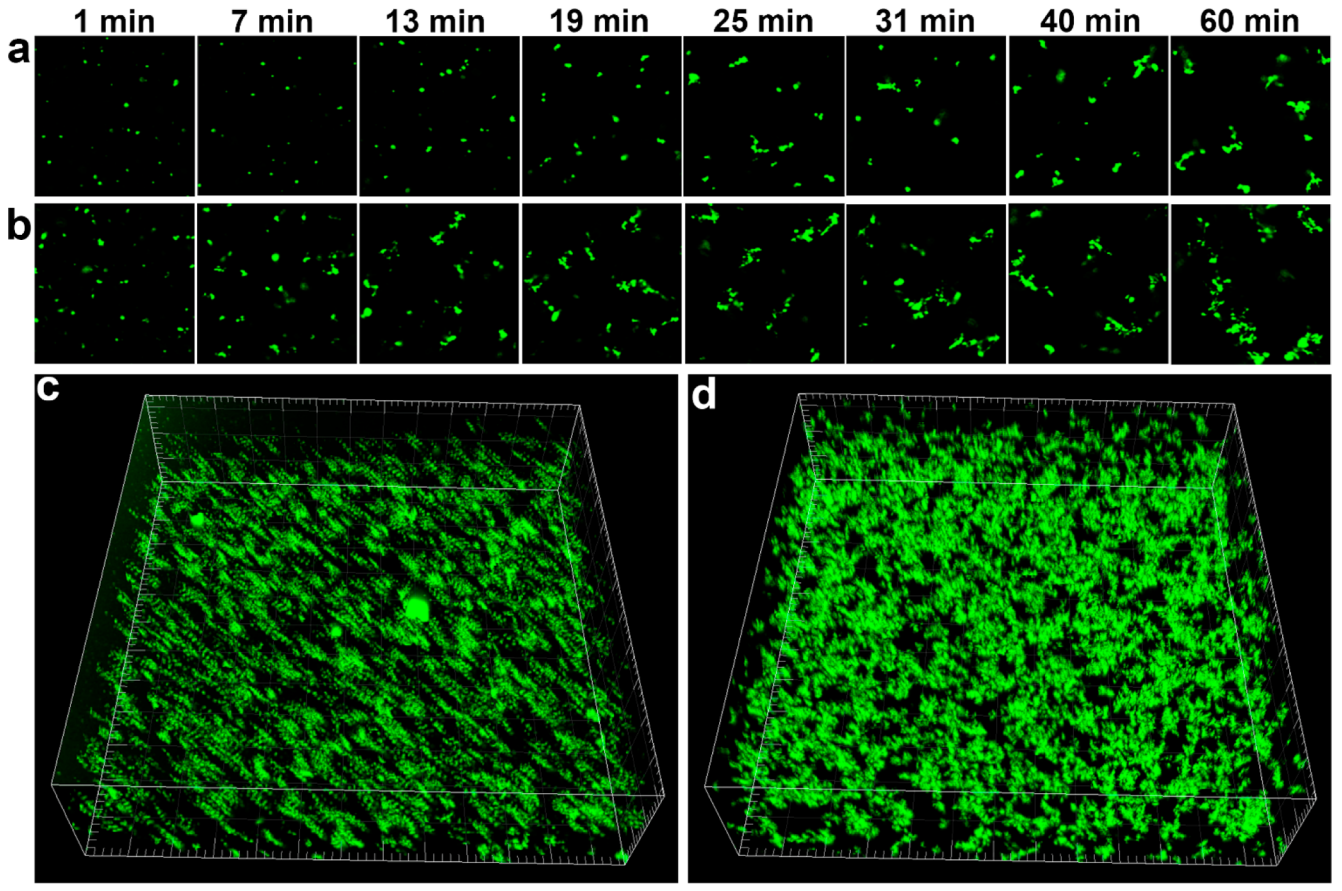

Figure 6. Dynamic morphology changes of fibrinogen treated with MB/Au-Closed-loop (a) and photo liberated thrombin (b). 3D Surface projections of Z-stack images at t = 60 min for fibrinogen treated with MB/Au-Closed-loop (c) and photo liberated thrombin (d).

DOI: 10.1021/jacs.5b04894
J. Am. Chem. Soc. 2015, 137, 10576−10584

measured to test the potential application of this strategy in regulation of thrombin activity in a biological sample. As shown in Table 2, the TCT of thrombin and TBA15-inhibited thrombin are 11.2 and 14.2 s, respectively, suggesting that thrombin activity is inhibited to some extent by TBA15. However, plasma samples treated with MB/Au-Closed-loop show TCT of 36.3 s, 2.2 times and 1.6 times longer than those of thrombin and TBA15-inhibited thrombin, respectively. These results demonstrate that the activity of thrombin trapped in the closed-loop structure is robustly inhibited and the inhibitory capabilities of the closed-loop structure outperform those of TBA15 by itself. After treatment with NIR light, the liberated thrombin gives a TCT of 13.8 s, indicating efficient restoration of thrombin activity. Additionally, the statistical significance between the above TCT values were analyzed (Table S11), and the results suggest that the above values give a valid representation of the inhibition and restoration of thrombin activity. The above results therefore highlight the future potential application of this strategy in regulation of thrombin activity in living systems.

Table 2. Thrombin Clotting Time (TCT)

samples	TCT (s)
Control	11.2 ± 0.5
TBA15-inhibited thrombin	14.2 ± 0.6
MB/Au-Closed-loop	36.3 ± 1.5
Photo liberated thrombin	13.8 ± 0.3

CONCLUSIONS

In this work, we have designed a novel strategy for regulation of protein activity by combining the advantages of proximity-dependent surface hybridization assay and the LSPR properties of noble metal nanoparticles. The activity of thrombin is efficiently inhibited by constructing a stable closed-loop structure to increase the binding affinity of aptamers toward thrombin. In the inhibition process, high specificity is obtained since aptamers are utilized as the affinity ligands and thrombin must be recognized by two aptamers in order to significantly inhibit catalytic activity. Furthermore, the activity of trapped thrombin can be efficiently restored by treating the closed-loop structure with NIR light to increase solution temperature to denature the 3D structures of aptamers and the double-helix structure of the closed-loop stem. The strategy described here exhibits great promise for application to thrombin activity regulation in real plasma samples. To conclude, this strategy can serve as a robust approach for protein activity regulation, and we anticipate that this strategy will find broad application in the study of the mechanisms of biological processes and metabolic pathway regulation.

EXPERIMENTAL SECTION

Preparation of AuNRs. AuNRs were synthesized via the seed-mediated growth method.[22] The gold seeds solution was prepared as follows. Typically, 0.25 mL of $HAuCl_4$ (0.01 M) was added to 9.75 mL of CTAB solution (0.1 M). Then, 600 μL of $NaBH_4$ (10 mM) precooled to 0 °C was quickly added to the above solution under vigorous stirring. The resulting gold nanoparticles were used as seeds for the synthesis of AuNRs. Briefly, 2 mL of $HAuCl_4$ (0.01 M) and 0.6 mL of $AgNO_3$ (0.01 M) were added to 38 mL of CTAB solution (0.1 M). After that, ascorbic acid (0.21 mL, 0.1 M) was added to the above solution under gentle shaking and the solution turned colorless. Finally, 0.12 mL of gold seeds solution was added to the above growth solution and the mixture was left at 37 °C overnight. The as-prepared AuNRs were centrifuged to remove excess CTAB and were further dispersed in water.

Binding-Induced DNA Strand Displacement Assay. Thiol-labeled TBA15 was added to an AuNR solution (TBA15/AuNR, 500:1) and the solution was allowed to react for 12 h at 37 °C. Then, TBA15-modified AuNRs (designated as Au-TBA15) were purified by centrifugation and the loaded amounts of TBA15 were determined with ultraviolet−visible spectroscopy. Au-TBA15 was further treated with 6-mercapto-1-hexanol (120 μM) for 2 h to passivate the active sites on the surface of AuNRs. The final solution was centrifuged to separate Au-TBA15 from the unreacted reagents. After that, FAM-DNA was added to the Au-TBA15 solution at 1:1 ratio. The mixture was heated to 70 °C for 5 min and allowed to cool to room temperature to form the TBA15/FAM-DNA duplex. The fluorescence intensity of the above sample was measured before and after the annealing process with excitation at 480 nm by a fluorescence spectrometer (Hitachi. Ltd., F-4600, Japan). TBA29 (TBA29/TBA15, 2:1) and thrombin (0.2 μM) was added separately to the above solution, and the mixtures were incubated for 2 h to test whether TBA29 or thrombin could initiate the strand displacement reaction. To verify the formation of the closed-loop structure, TBA29 (TBA29/TBA15, 2:1) and thrombin (0−0.3 μM) were added simultaneously to the TBA15/FAM-DNA duplex solution. After incubation for 2 h, the fluorescence intensities were measured on a fluorescence spectrometer.

Preparation of MB/AuNRs Nanoparticles. Magnetic beads modified with carboxyl groups (40 μL, 10 mg/mL) were dispersed in 1.5 mL of MES buffer (10 mM, pH 6.0, 150 mM NaCl). To this solution, 8 mg of EDC and 1.2 mg of NHS were added, and the solution was incubated at 37 °C for 15 min with gentle shaking. The activated MBs were separated with a magnet and dispersed in 400 μL of PBS buffer (pH 7.4, 150 mM NaCl). Then, 400 μL of 1 mM cysteine was added to the solution and the mixture was incubated at 37 °C for 24 h. The cysteine-functionalized MBs were separated with a permanent magnet and then washed 3 times with 400 μL of PBS buffer. After that, the as prepared MBs were dispersed in 1 mL of AuNRs solution and the mixture was allowed to react for 24 h. Finally, the resultant MB/AuNRs were separated with a magnet and the particles were dispersed in 1 mL of PBS buffer.

Measurement of the Photothermal Properties of MB/Au. MB/Au solution (0.5 mL, 0.4 mg/mL) was placed in a plastic centrifuge tube (2 mL) at ambient temperature. The solution was then exposed to an 808 nm CW laser with tunable energy density, and the temperature of the solution was measured without stirring by using a calibrated thermocouple device inserted into the solution. The final temperature can be fine-tuned by simply changing the energy density of the laser.

Preparation of Close-Loop, Au-Closed-Loop, and MB/Au-Closed-Loop Structures. The principle of this experiment involves binding of TBA15 and TBA29 to thrombin at different binding sites, followed by hybridization of the proximity ligands on TBA15 and TBA29 to form a closed-loop structure around the thrombin molecule. Taking the preparation of Closed-loop structure as an example, typically, 2 μL of TBA29 (1 μM), 1 μL of TBA15 (1 μM) and 1 μL of thrombin (0.1 μM) were mixed in 200 μL of Tris-HCl buffer (25 mM, pH 7.4, 150 mM NaCl, 5.0 mM KCl, 1.0 mM $MgCl_2$, 1.0 mM $CaCl_2$), and the solution was incubated at room temperature for 30 min. Au-Closed-loop and MB/Au-Closed-loop structures were prepared with the same procedure except that TBA15 functionalized AuNRs or MB/Au were utilized instead of TBA15. The concentrations of TBA15, Au-TBA15 (counted by TBA15), MB/Au-TBA15 (counted by TBA15), TBA29 and thrombin were kept constant. The inhibition efficiencies of the closed-loop structures toward thrombin were compared to those of TBA15 and TBA29 at the same concentrations, and the added amount of thrombin was also the same.

Liberation of Thrombin Trapped in MB/Au-Closed-Loop. The principle of this experiment was that the MB/Au-Closed-loop could be disrupted by increasing the temperature to denature the 3D structure of TBA15, TBA29 and the DNA duplex formed by the

DOI: 10.1021/jacs.5b04894
J. Am. Chem. Soc. 2015, 137, 10576−10584

proximity ligands. MB/Au-Closed-loop solution (0.5 mL) was heated to different temperatures (40, 50, 60, 70, 80 °C) for 10 min and the MB/Au-TBA15 were instantly separated with a permanent magnet. Similarly, 0.5 mL of MB/Au-Closed-loop solution was exposed to the 808 nm CW laser with energy density of 1.055 W/cm^2. The temperature of the solution rapidly increased to 60 °C and the solution was kept at this temperature for 10 min. Then, MB/Au-TBA15 were also magnetically separated to release the thrombin.

Real-Time Monitoring of the Clotting Reactions by Light Scattering Measurements. The underlying principle of this experiment is that thrombin can catalyze the conversion of fibrinogen into insoluble fibrin, which results in an increase of the scattered light intensity. As a result, the clotting reaction can be easily monitored by the increase of scattered light intensity from the sample cell with a fluorescence spectrometer. Typically, 5 μL of fibrinogen (10 mg/mL) was quickly added to 200 μL of TBA15-inhibited thrombin, TBA29-inhibited thrombin, Closed-loop, Au-Closed-loop, MB/Au-Closed-loop or the liberated thrombin solution. The scattering intensities were measured as a function of time on a fluorescence spectrophotometer at 650 nm. The clotting reaction catalyzed by pure thrombin was always measured together with other samples to serve as an internal standard. All of the clotting times were normalized based on the standards.

In Situ Monitoring the Clotting Reactions with LSCM. To verify the inhibition and liberation of thrombin activity, the conversion of fluorescent fibrinogen into visible fibrin fibers was monitored. In a typical experiment, Alexa Fluor 488 labeled fibrinogen solution (1 μL, 10 mg/mL) was added to separate 50 μL samples of thrombin, TBA15-inhibited thrombin, Closed-loop, Au-Closed-loop, MB/Au-Closed-loop or the liberated thrombin solutions. Then, 30 μL of each solution was instantly dropped on the bottom of a small Petri dishes and a coverslip was carefully placed on the liquid drop. The images were obtained every 2 min with the excitation by a 488 nm laser until the reactions were complete. Z-stack images of each sample were taken at 60 min. All of the mages were acquired using a 20× dry objective.

Human Plasma Tests. To further test whether this strategy can be applied to thrombin activity regulation in real samples, the TCTs of thrombin, TBA15-inhibited thrombin, Closed-loop, Au-Closed-loop, MB/Au-Closed-loop or the liberated thrombin solutions were determined using human plasma. Reaction solutions were prepared as described above for the clotting tests, except that the initial thrombin time was monitored on an automatic coagulation analyzer. Blood from healthy volunteers (3 mL) was mixed with sodium citrate solution (333 μL, 0.109 M) and was further centrifuged at 3000 rpm for 3 min to remove blood cells. To a standard glass bottle were added 1 mL of PBS buffer and 200 μL of the reaction mixtures described above. For TCT determination, the scattering intensity was monitored until the plateau was reached. The clotting time was determined to be the first point at the half peak width.

■ ASSOCIATED CONTENT

Supporting Information

The Supporting Information is available free of charge on the ACS Publications website at DOI: 10.1021/jacs.5b04894.

Movie S1 (AVI)
Movie S2 (AVI)
Movie S3 (AVI)
Movie S4 (AVI)
TEM images of AuNRs, MB and MB/Au, LSCM images, average intensity of LSCM images, zeta potential measurement, degree of fibrinogen cleavage, LM images, background scattering of AuNRs and AuNR-MBs, cyclical modulation of thrombin activity, TCT measurement and the statistical significance analysis (PDF)

■ AUTHOR INFORMATION

Corresponding Author

* yuanquan@whu.edu.cn

Author Contributions

§J. Wang and Y. Wei contributed equally to this work.

Notes

The authors declare no competing financial interest.

■ ACKNOWLEDGMENTS

This work was supported by the National Natural Science Foundation of China (21201133, 51272186, 21422105) and the Fundamental Research Funds for the Central Universities (2014203020205). Q. Yuan thanks the large-scale instrument and equipment sharing foundation of Wuhan University.

■ REFERENCES

(1) Petsko, G. A.; Ringe, D. Control of Protein Function. In *Protein Structure and Function*; Lawrence, E., Robertson, M., Eds.; New Science Press Ltd: London, 2004; pp 86−126.

(2) (a) Wells, J. A.; McClendon, C. L. *Nature* **2007**, *450*, 1001−1009. (b) Tzeng, S.-R.; Kalodimos, C. G. *Nature* **2012**, *488*, 236−240. (c) Bialy, L.; Waldmann, H. *Angew. Chem., Int. Ed.* **2005**, *44*, 3814−3839. (d) Volgraf, M.; Gorostiza, P.; Numano, R.; Kramer, R. H.; Isacoff, E. Y.; Trauner, D. *Nat. Chem. Biol.* **2006**, *2*, 47−52. (e) Zhang, F.; Zarrine-Afsar, A.; Al-Abdul-Wahid, M. S.; Prosser, R. S.; Davidson, A. R.; Woolley, G. A. *J. Am. Chem. Soc.* **2009**, *131*, 2283−2289.

(3) (a) Arkin, M. R.; Wells, J. A. *Nat. Rev. Drug Discovery* **2004**, *3*, 301−317. (b) Arkin, M. R.; Tang, Y.; Wells, J. A. *Chem. Biol.* **2014**, *21*, 1102−1114.

(4) (a) Kim, Y.; Cao, Z.; Tan, W. *Proc. Natl. Acad. Sci. U. S. A.* **2008**, *105*, 5664−5669. (b) Best, J. L.; Amezcua, C. A.; Mayr, B.; Flechner, L.; Murawsky, C. M.; Emerson, B.; Zor, T.; Gardner, K. H.; Montminy, M. *Proc. Natl. Acad. Sci. U. S. A.* **2004**, *101*, 17622−17627. (c) Buckley, D. L.; Gustafson, J. L.; Van Molle, I.; Roth, A. G.; Tae, H. S.; Gareiss, P. C.; Jorgensen, W. L.; Ciulli, A.; Crews, C. M. *Angew. Chem., Int. Ed.* **2012**, *51*, 11463−11467. (d) Guo, W.; Wisniewski, J. A.; Ji, H. *Bioorg. Med. Chem. Lett.* **2014**, *24*, 2546−2554. (e) Han, D.; Zhu, Z.; Wu, C.; Peng, L.; Zhou, L.; Gulbakan, B.; Zhu, G.; Williams, K. R.; Tan, W. *J. Am. Chem. Soc.* **2012**, *134*, 20797−20804. (f) Joachimi, A.; Mayer, G.; Hartig, J. S. *J. Am. Chem. Soc.* **2007**, *129*, 3036−3037.

(5) Lawrence, D. S. *Curr. Opin. Chem. Biol.* **2005**, *9*, 570−575.

(6) Wenck, K.; Koch, S.; Renner, C.; Sun, W.; Schrader, T. *J. Am. Chem. Soc.* **2007**, *129*, 16015−16019.

(7) (a) Xing, H.; Hwang, K.; Li, J.; Torabi, S. F.; Lu, Y. *Curr. Opin. Chem. Eng.* **2014**, *4*, 79−87. (b) Zheng, D.; Seferos, D. S.; Giljohann, D. A.; Patel, P. C.; Mirkin, C. A. *Nano Lett.* **2009**, *9*, 3258−3261. (c) Zuo, X.; Song, S.; Zhang, J.; Pan, D.; Wang, L.; Fan, C. *J. Am. Chem. Soc.* **2007**, *129*, 1042−1043. (d) Liu, H.; Xiang, Y.; Lu, Y.; Crooks, R. M. *Angew. Chem., Int. Ed.* **2012**, *51*, 6925−6928. (e) Liang, H.; Zhang, X.-B.; Lv, Y.; Gong, L.; Wang, R.; Zhu, X.; Yang, R.; Tan, W. *Acc. Chem. Res.* **2014**, *47*, 1891−1901. (f) Fang, X.; Tan, W. *Acc. Chem. Res.* **2010**, *43*, 48−57. (g) Lu, X. G.; Watts, E.; Jia, F.; Tan, X. Y.; Zhang, K. *J. Am. Chem. Soc.* **2014**, *136*, 10214−10217. (h) Giljohann, D. A.; Mirkin, C. A. *Nature* **2009**, *462*, 461−464. (i) Li, D.; Song, S.; Fan, C. *Acc. Chem. Res.* **2010**, *43*, 631−641. (j) Liu, J.; Cao, Z.; Lu, Y. *Chem. Rev.* **2009**, *109*, 1948−1998. (k) Tan, X. Y.; Li, B. B.; Lu, X. G.; Jia, F.; Santori, C.; Menon, P.; Li, H.; Zhang, B. H.; Zhao, J. J.; Zhang, K. *J. Am. Chem. Soc.* **2015**, *137*, 6112−6115.

(8) (a) Jayasena, S. D. *Clin. Chem.* **1999**, *45*, 1628−1650. (b) Song, S.; Wang, L.; Li, J.; Fan, C.; Zhao, J. *TrAC, Trends Anal. Chem.* **2008**, *27*, 108−117. (c) Tan, W.; Wang, H.; Chen, Y.; Zhang, X.; Zhu, H.; Yang, C.; Yang, R.; Liu, C. *Trends Biotechnol.* **2011**, *29*, 634−640.

(9) Bock, L. C.; Griffin, L. C.; Latham, J. A.; Vermaas, E. H.; Toole, J. J. *Nature* **1992**, *355*, 564−566.

(10) (a) Fredriksson, S.; Gullberg, M.; Jarvius, J.; Olsson, C.; Pietras, K.; Gústafsdóttir, S. M.; Östman, A.; Landegren, U. *Nat. Biotechnol.* **2002**, *20*, 473−477. (b) Schallmeiner, E.; Oksanen, E.; Ericsson, O.; Spångberg, L.; Eriksson, S.; Stenman, U. H.; Pettersson, K.; Landegren, U. *Nat. Methods* **2007**, *4*, 135−137.

DOI: 10.1021/jacs.5b04894
J. Am. Chem. Soc. 2015, 137, 10576−10584

(11) Söderberg, O.; Gullberg, M.; Jarvius, M.; Ridderstråle, K.; Leuchowius, K. J.; Jarvius, J.; Wester, K.; Hydbring, P.; Bahram, F.; Larsson, L. G. *Nat. Methods* **2006**, *3*, 995−1000.
(12) (a) Zhang, H.; Wang, Z.; Li, X. F.; Le, X. C. *Angew. Chem., Int. Ed.* **2006**, *45*, 1576−1580. (b) Li, F.; Zhang, H.; Lai, C.; Li, X. F.; Le, X. C. *Angew. Chem., Int. Ed.* **2012**, *51*, 9317−9320. (c) Zhang, H.; Li, F.; Dever, B.; Wang, C.; Li, X. F.; Le, X. C. *Angew. Chem., Int. Ed.* **2013**, *52*, 10698−10705. (d) Zhang, H.; Li, F.; Dever, B.; Li, X.-F.; Le, X. C. *Chem. Rev.* **2013**, *113*, 2812−2841.
(13) Zhang, H.; Li, X.-F.; Le, X. C. *Anal. Chem.* **2012**, *84*, 877−884.
(14) Zhou, C.; Yang, Z.; Liu, D. *J. Am. Chem. Soc.* **2012**, *134*, 1416−1418.
(15) (a) Schierling, B.; Noël, A.-J.; Wende, W.; Volkov, E.; Kubareva, E.; Oretskaya, T.; Kokkinidis, M.; Römpp, A.; Spengler, B.; Pingoud, A. *Proc. Natl. Acad. Sci. U. S. A.* **2010**, *107*, 1361−1366. (b) Li, H.; Hah, J.-M.; Lawrence, D. S. *J. Am. Chem. Soc.* **2008**, *130*, 10474−10475. (c) Kohse, S.; Neubauer, A.; Pazidis, A.; Lochbrunner, S.; Kragl, U. *J. Am. Chem. Soc.* **2013**, *135*, 9407−9411. (d) Kim, Y.; Phillips, J. A.; Liu, H.; Kang, H.; Tan, W. *Proc. Natl. Acad. Sci. U. S. A.* **2009**, *106*, 6489−6494. (e) Heckel, A.; Buff, M. C.; Raddatz, M. S. L.; Müller, J.; Pötzsch, B.; Mayer, G. *Angew. Chem., Int. Ed.* **2006**, *45*, 6748−6750. (f) Heckel, A.; Mayer, G. *J. Am. Chem. Soc.* **2005**, *127*, 822−823. (g) Karginov, A. V.; Zou, Y.; Shirvanyants, D.; Kota, P.; Dokholyan, N. V.; Young, D. D.; Hahn, K. M.; Deiters, A. *J. Am. Chem. Soc.* **2011**, *133*, 420−423.
(16) Mayer, G.; Heckel, A. *Angew. Chem., Int. Ed.* **2006**, *45*, 4900−4921.
(17) Izquierdo-Serra, M.; Gascon-Moya, M.; Hirtz, J. J.; Pittolo, S.; Poskanzer, K. E.; Ferrer, È.; Alibes, R.; Busque, F.; Yuste, R.; Hernando, J. *J. Am. Chem. Soc.* **2014**, *136*, 8693−8701.
(18) de Puig, H.; Rius, A. C.; Flemister, D.; Baxamusa, S. H.; Schifferli, K. H. *PLoS One* **2013**, *8*, e68511.
(19) (a) Liz-Marzán, L. M.; Murphy, C. J.; Wang, J. *Chem. Soc. Rev.* **2014**, *43*, 3820−3822. (b) Chen, H.; Shao, L.; Li, Q.; Wang, J. *Chem. Soc. Rev.* **2013**, *42*, 2679−2724.
(20) (a) Tasset, D. M.; Kubik, M. F.; Steiner, W. *J. Mol. Biol.* **1997**, *272*, 688−698. (b) Shiang, Y. C.; Huang, C. C.; Wang, T. H.; Chien, C. W.; Chang, H. T. *Adv. Funct. Mater.* **2010**, *20*, 3175−3182.
(21) Wang, S. X.; Zhou, Y.; Yang, S. C.; Ding, B. J. *Colloids Surf., B* **2008**, *67*, 122−126. Saptarshi, S. R.; Duschl, A.; Lopata, A. L. *J. Nanobiotechnol.* **2013**, *11*, 26.
(22) Murphy, C. J.; Sau, T. K.; Gole, A. M.; Orendorff, C. J.; Gao, J.; Gou, L.; Hunyadi, S. E.; Li, T. *J. Phys. Chem. B* **2005**, *109*, 13857−13870.

DOI: 10.1021/jacs.5b04894
J. Am. Chem. Soc. 2015, 137, 10576−10584